Cbln2 and Cbln4 are expressed in distinct medial habenula-interpeduncular projections and contribute to different behavioral outputs

Erica Seigneur[a,b], Jai S. Polepalli[a,b], and Thomas C. Südhof[a,b,1]

[a]Department of Molecular and Cellular Physiology, Stanford University Medical School, Stanford, CA 94305; and [b]Howard Hughes Medical Institute, Stanford University Medical School, Stanford, CA 94305

Contributed by Thomas C. Südhof, August 20, 2018 (sent for review June 27, 2018; reviewed by Thomas Biederer, Craig M. Powell, and Susanne Schoch McGovern)

Cerebellins are important neurexin ligands that remain incompletely understood. Two critical questions in particular remain unanswered: do different cerebellins perform distinct functions, and do these functions act in the initial establishment of synapses or in rendering nascent synapses capable of normal synaptic transmission? Here we show that in mice, Cbln2 and Cbln4 are expressed in the medial habenula (MHb) nucleus in different types of neurons that project to distinct target neurons in the interpeduncular nucleus. Conditional genetic deletion of Cbln2 in the MHb impaired synaptic transmission at Cbln2$^+$ synapses in the interpeduncular neurons within 3 wk, but decreased synapse numbers only after 3 mo, suggesting a functional, but not a structural, requirement for Cbln2 in synapses formed by Cbln2-expressing neurons. In contrast, genetic deletions of Cbln4 in the MHb had no major effect on synaptic transmission or synapse numbers in interpeduncular target neurons. Nevertheless, MHb ablation of both Cbln2 and Cbln4 significantly impaired behavioral responses in mice, but affected different types of behaviors. Specifically, Cbln2 MHb deletions decreased spatial learning, as measured in the water T-maze, whereas Cbln4 MHb deletions increased anxiety levels, as monitored in the open field test and elevated plus maze. Thus, Cbln2 and Cbln4 are expressed in distinct MHb neurons that contribute to different behaviors.

synapse | neurexin | cerebellin | memory | synaptogenesis

The habenular complex, an important brain region linking the limbic forebrain to the midbrain, comprises two anatomically and functionally distinct nuclei, the lateral habenula (LHb) and medial habenula (MHb) (1–3). Input to the MHb arises primarily from the hippocampal formation and the amygdala. Most information transfer from the hippocampus to the MHb occurs via the lateral, medial, and posterior septal nuclei (the septofimbrial and triangular nuclei), the nucleus of the diagonal band, and the bed nucleus of the stria terminalis (BNST), whereas most information transfer from the amygdala to the MHb is mediated by the BNST and the bed nucleus of the anterior commissure (4–8). Axons from the MHb form the internal portion of the fasciculus retroflexus and terminate almost exclusively in the midbrain in the interpeduncular nucleus (IPN) (2, 9). The IPN in turn projects predominantly to the dorsal raphe, hippocampus, medial septum, and entorhinal cortex (10–14).

The MHb contains ventral (vMHb) and dorsal (dMHb) subdivisions. Recent lesion experiments and genetic studies in mice and zebrafish suggested that these regions are functionally distinct, with the vMHb regulating anxiety (8, 15, 16) and the dMHb regulating fear acquisition and avoidance learning (8, 17). Furthermore, in classic lesion studies in rats, ablation of the MHb or the fasciculus retroflexus impaired spatial learning (18–20) and active avoidance learning (21, 22). In addition, lesions of the IPN resulted in impaired landmark and path integration navigation without affecting beacon navigation (23). While these studies demonstrated the functional importance of the MHb, they represent relatively blunt manipulations of the entire MHb. Because of the small size and complex nature of the MHb, identifying functionally relevant genes will be essential for a more precise functional dissection of its subnuclei than can be achieved with lesions or similar manipulations.

The cerebellins constitute a family of secreted proteins (Cbln1–Clbn4) that, except for Cbln3, are expressed not only in cerebellum, but throughout the brain (24–29). Cbln1, Cbln2, and Cbln4 function as autonomous homohexamers and are abundantly expressed in subsets of neurons throughout the brain (26–29); however, Cbln3 is unable to assemble into homohexamers and can only be exported from a neuronal endoplasmic reticulum in a heterohexameric complex with Cbln1 (24, 25). Cerebellins act as synaptic adaptors by binding simultaneously to presynaptic neurexins (all cerebellins) and postsynaptic GluRδs (Cbln1 and Cbln2) (30–35) or to DCC (deleted in colorectal cancer) and neogenin-1 (Cbln4) (36, 37). The neurexin/cerebellin/GluRδ complex forms a transsynaptic cell-adhesion complex, but whether DCC and neogenin are presynaptic or postsynaptic is unclear. Thus, it remains unknown whether a transsynaptic neurexin-Cbln4-DCC/neogenin complex exists or whether a different postsynaptic receptor for Cbln4 is involved.

Cerebellins only bind to neurexin variants containing an insert in their alternatively spliced sequence 4 (SS4) (31–33). The brain expresses three principal neurexin genes (Nrxn1–Nrxn3) that encode both longer α-neurexins and shorter β-neurexins (38–40). Neurexins are extensively alternatively spliced at six canonical sites (41–43). Of these alternatively spliced sequences, the insert or

Significance

Cerebellins are important neurexin ligands that remain poorly understood. Two critical questions in particular remain unanswered: do different cerebellins perform distinct functions, and do these functions act in the initial establishment of synapses or in rendering nascent synapses capable of normal synaptic transmission? Here we report that in mice, two homologous cerebellins, Cbln2 and Cbln4, are expressed in different types of neurons of the medial habenula (MHb), and that these neurons project to distinct target neurons in the interpeduncular nucleus. Ablation of Cbln2 or Cbln4 from the MHb impairs distinct behaviors, but only ablation of Cbln2 affects synapse numbers. Our data show that different cerebellins perform distinct functions that involve synaptic information processing but not initial synapse formation.

Author contributions: E.S. and T.C.S. designed research; E.S. and J.S.P. performed research; E.S., J.S.P., and T.C.S. analyzed data; and E.S. and T.C.S. wrote the paper.

Reviewers: T.B., Tufts University; C.M.P., University of Alabama at Birmingham; and S.S.M., University of Bonn.

The authors declare no conflict of interest.

[1]To whom correspondence should be addressed. Email: tcs1@stanford.edu.

This article contains supporting information online at www.pnas.org/lookup/suppl/doi:10.1073/pnas.1811086115/-/DCSupplemental.

Published online October 4, 2018.

deletion of a 30-aa sequence at SS4 may be particularly important because it regulates neurexin binding not only to cerebellins, but also to multiple other ligands (31–33, 44).

Cerebellins are thought to function as bidirectional synaptic organizers in many brain regions, as best characterized by the role of Cbln1 in the cerebellum (reviewed in ref. 45). Here deletion of *Cbln1* results in an ∼40% loss of parallel fiber-Purkinje cell synapses and abolishes long-term depression in the surviving synapses (46–48). The precise function of cerebellins remains unclear, however. Even in the cerebellum, deletion of Cbln1 leads to elimination of only a subset of parallel fiber synapses but affects the function of all synapses, suggesting a role for cerebellins not in the establishment of synapses, but in their functional organization.

We recently generated Cbln2 and Cbln4 reporter and conditional KO mice, which allowed us to map the expression of Cbln2 and Cbln4 in selected brain regions (29). We found that constitutive deletions of cerebellins in mice, although not lethal, caused significant behavioral impairment and led to a delayed loss of synapses in several brain regions (48). In the present study, we observed a particularly strong expression pattern of Cbln2 and Cbln4 in the MHb, with Cbln2 and Cbln4 differentially synthesized in the dMHb and vMHb, respectively (Fig. 1*A*).

Given this expression pattern, we hypothesized that the conditionally mutant Cbln2 and Cbln4 mice could provide a tool for testing whether Cbln2 and Cbln4 perform similar or different functions, and whether these functions are related to the formation or the functional organization of synapses. Moreover, we realized that these mice may enable identification of the unique functions of the dMHb and vMHb, and thus we used Cre-recombinase to selectively delete Cbln2 or Cbln4 in the MHb. Our experiments demonstrate that Cbln2-expressing neurons in the dMHb regulate passive avoidance learning, spatial learning, and short-term memory, while Cbln4-expressing neurons in the vMHb regulate anxiety. In addition, we found that loss of Cbln2 in the MHb results in a decreased miniature EPSC (mEPSC) frequency in the lateral IPN, followed by a delayed selective loss of vGluT1$^+$ synapses. Taken together, our results demonstrate that the MHb is functionally divided into dorsal and ventral subnuclei, and that Cbln2 and Cbln4 act as important regulators of dMHb and vMHb function, respectively.

Results

Cerebellins and Their Binding Partners Are Highly Expressed in MHb Neurons Projecting to the IPN. In characterizing the expression profiles of Cbln2 and Cbln4 in the habenula with Cbln2-mVenus and Cbln4-mVenus reporter mice (29), we observed intensely labeled Cbln2$^+$ neurons in the MHb with a few additional Cbln2$^+$ neurons in the LHb, and detected dense Cbln2$^+$ fibers projecting from the MHb to the IPN via the fasciculus retroflexus (Fig. 1 *B* and *D*). Moreover, we also observed intensely labeled Cbln4$^+$ neurons in the MHb, again with Cbln4$^+$ axons extending from the MHb to the IPN via the fasciculus retroflexus; however, in contrast to Cbln2$^+$ neurons, no Cbln4$^+$ neurons were observed in the LHb (Fig. 1 *C* and *E*).

To confirm and extend these initial morphological findings, we measured the mRNA levels of cerebellins and their binding partners in the habenula and the IPN using quantitative RT-PCR (qRT-PCR). Transcript levels were normalized to those of the housekeeping gene β-actin and are presented in percentage of β-actin levels. We found that Cbln1, Cbln2, and Cbln4 were abundantly expressed in the habenular complex (lateral and medial Hb), at ∼5% (Cbln1 and Cbln4) and ∼20% (Cbln2) of β-actin levels (Fig. 1*F*). Previous research using RNA in situ hybridization revealed Cbln1 expression in the LHb but not in the MHb (26, 28); therefore, the mRNA levels that we measured in the habenular complex likely reflect the expression of Cbln1 in the LHb, of Cbln2 in both the LHb and MHb, and of Cbln4 only in the MHb.

Based on previous studies in the cerebellum (30, 31), cerebellins are thought to be presynaptically coexpressed with neurexins. Consistent with this conclusion, Nrxn1, Nrxn2, and Nrxn3 were abundantly produced in the habenular complex, at ∼10% (Nrxn1), ∼8% (Nrxn2), and ∼3% (Nrxn3) of β-actin levels (Fig. 1*F*). Alternative splicing of neurexins at SS4 is region-specific, and some brain regions, including the cerebellum, primarily synthesize +SS4 isoforms of all three neurexins (49). Because cerebellins are abundantly expressed in the habenular complex and only bind to +SS4 variants of neurexins (31–34), we hypothesized that the majority of habenular neurexins represent +SS4 variants. To test this, we measured the relative expression of +SS4 to −SS4 neurexin isoforms using a semiquantitative RT-PCR assay. Indeed, +SS4 isoforms of all three neurexins were expressed predominately and accounted for ∼68% of Nrxn1, ∼78% of Nrxn2, and ∼93% of Nrxn3 mRNAs (Fig. 1*G*).

Finally, we measured the mRNA levels of putative postsynaptic cerebellin-binding partners in the IPN. *Grid1* and *Grid2* (which encode GluRδ1 and GluRδ2, respectively) were modestly expressed in the IPN, with *Grid1* and *Grid2* mRNAs present at ∼1% of β-actin levels. In contrast, the Cbln4-binding partners *DCC* and *NEO1* were detected at ∼4% and 22% of β-actin levels, respectively (Fig. 1*H*). Taken together, these results suggest that habenular Cbln2 and Cbln4 that are coexpressed with +SS4 neurexins can mediate transsynaptic interactions between the MHb and the IPN by binding to GluRδ1/2 and DCC/neogenin, respectively.

Expression of Cbln2 and Cbln4 Is Enriched in Distinct Subnuclei Within the MHb. The MHb is broadly divided into a vMHb containing primarily cholinergic neurons and a dMHb containing primarily neurons expressing substance P (SubP) (3, 9). Based on topography and morphology, the dMHb is further divided into two subnuclei, termed dorsal MHb (dMHbD) and superior MHb (dMHbS), and the vMHb is further divided into four subnuclei: lateral (vMHbL), central (vMHbC), medial (vMHbM), and intermediate ventral MHb (vMHbI) (3, 50–52). A recent study also identified a subnucleus, termed region X (HbX), that appears to contain a mix of MHb and LHb neurons (52).

Cbln2 expression was observed throughout the MHb, but the intensity of the mVenus signal was significantly greater in the dMHbD, dMHbS, and HbX subregions than in the ventral regions (Fig. 2*A*). Conversely, Cbln4 was highly expressed in the vMHbL, vMHbC, vMHbM, and vMHbI subregions; weakly expressed in the dMHbS; and absent from the dMHbD and HbX (Fig. 2*C*).

To further characterize the neuronal profile of the Cbln2- and Cbln4-expressing neurons in the MHb, we conducted colabeling experiments using antibodies against the vesicular acetylcholine transporter (VAChT), SubP, calbindin, and calretinin that mark different neuronal subpopulations. We found that expression of VAChT was restricted to the vMHbL, vMHbC, vMHbM, and vMHbI subregions (*SI Appendix*, Fig. S1); Cbln2 was weakly expressed in a subset of VAChT$^+$ neurons (Fig. 2*A*), whereas Cbln4 was highly expressed in nearly all VAChT$^+$ neurons (Fig. 2 *C* and *D*). SubP expression was restricted to the dMHbD and dMHbS subregions (*SI Appendix*, Fig. S1) and was highly colocalized with Cbln2 (Fig. 2 *A* and *B*) but not with Cbln4 (Fig. 2*C*). Calbindin expression was restricted to the dMHbD, the superior portion of vMHbL, and HbX (*SI Appendix*, Fig. S1) and was highly colocalized with Cbln2 (Fig. 2 *A* and *B*) but not with Cbln4 (Fig. 2 *C* and *D*). Finally, calretinin expression was restricted to the dMHbD, dMHbS, and a small portion of HbX (*SI Appendix*, Fig. S1) and was highly colocalized with Cbln2 in all three regions (Fig. 2 *A* and *B*). Calretinin expression was also observed in dMHbS neurons that weakly expressed Cbln4 (Fig. 2*C*).

Similar to the segregation observed in the MHb, we found that axons from cholinergic and SubP-expressing neurons project to nonoverlapping subregions in the IPN. Specifically, cholinergic axons terminate in the central (IPC) and rostral (IPR) subnuclei, whereas SubP-expressing axons terminate primarily in the lateral (IPL) subnuclei and partially in the IPR (9). Consistent with

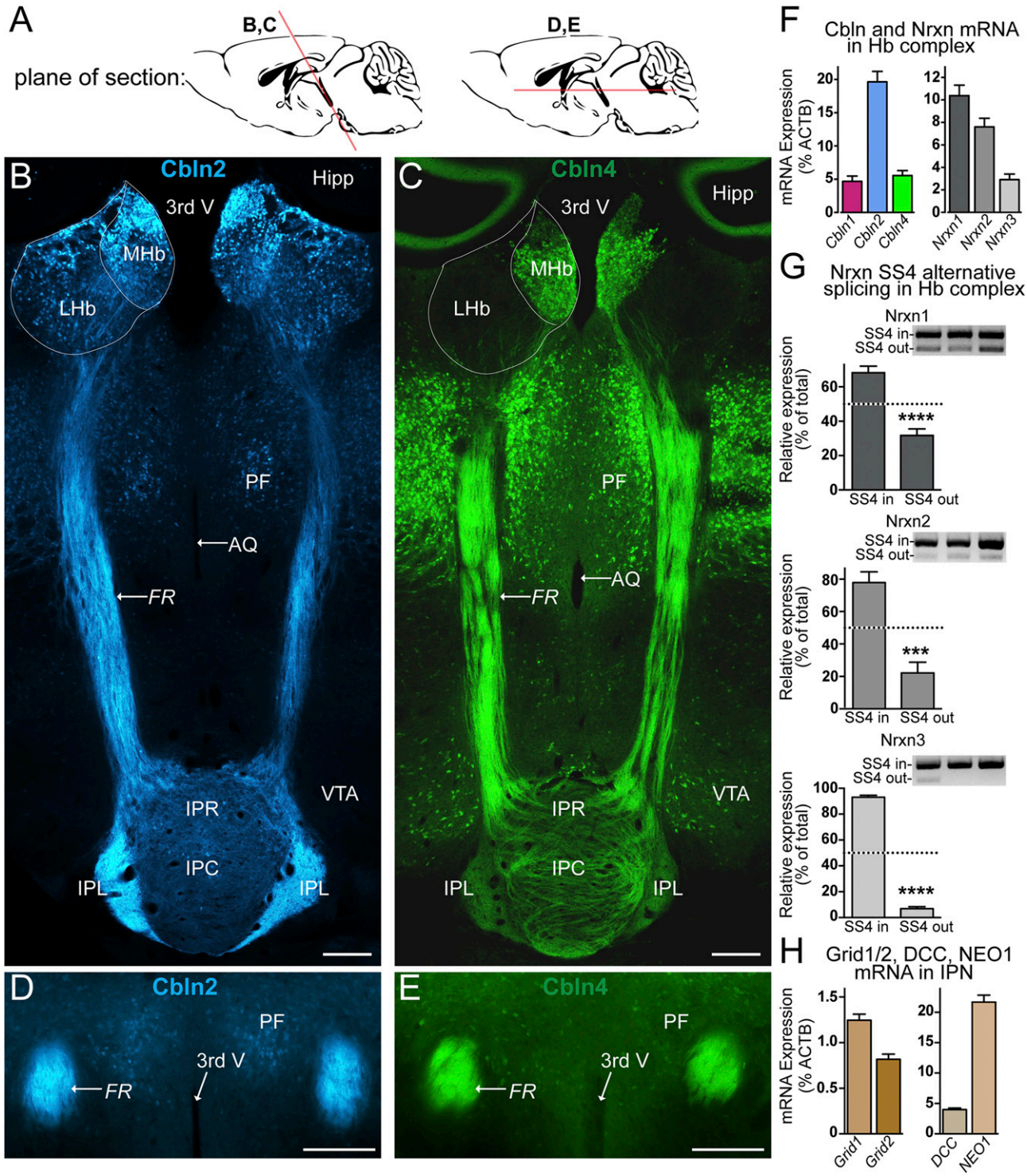

Fig. 1. Projection of neurons of the MHb expressing Cbln2 and Cbln4 to the IPL and IPC, respectively. (*A*) Schematic showing the approximate location and sectioning angle of the images shown in *B* and *C* (*Left*) and in *D* and *E* (*Right*). (*B* and *C*) Coronal section, cut at an angle, from Cbln2-mVenus (*B*) or Cbln4-mVenus (*C*) reporter mice. Cbln2$^+$ neurons are seen in the LHb and MHb, while Cbln4$^+$ neurons are observed only in the MHb. Axons from Cbln2$^+$ and Cbln4$^+$ MHb neurons form the fasciculus retroflexus (FR) and terminate in the IPR and IPL and in the IPR and IPC subregions, respectively. (Scale bar: 200 μm.) (*D* and *E*) Horizontal sections from Cbln2-mVenus (*D*) and Cbln4-mVenus (*E*) reporter mice showing strong expression of Cblns in the FR. (Scale bar: 200 μm.) (*F*) Expression of Cbln1, Cbln2, and Cbln4 (*Left*) and of Nrxn1, Nrxn2, and Nrxn3 (*Right*) mRNAs in the habenular complex (includes the LHb and MHb). mRNAs were quantified by qRT-PCR using total RNA extracted from tissue lysates and were normalized to β-actin. (*G*) Expression in the habenular complex of Nrxn variants with (+SS4) or without (−SS4) an insert at alternative SS4. mRNAs were measured by semiquantitative RT-PCR using the same total RNA samples as in *F*; PCR products were analyzed by gel electrophoresis; sample images of triplicate experiments are shown above the bar graphs. Results are displayed as percent of total. Data were analyzed by Student's *t* test. ***$P = 0.0001$; ****$P < 0.0001$. (*H*) Expression of Grid1, Grid2, DCC, and NEO1 mRNAs in the IPN as measured by qRT-PCR and normalized to β-actin. Grid1 and Grid2 encode for GluRδ1 and GluRδ2, respectively, and form a complex with Cbln1 or Cbln2 and neurexins, whereas DCC and NEO1 bind to Cbln4. Data in F–H are mean ± SEM ($n = 6$ mice). 3V, third ventricle; AQ, cerebral aqueduct; Hipp, hippocampus; PF, parafascicular nucleus of the thalamus; VTA, ventral tegmental area.

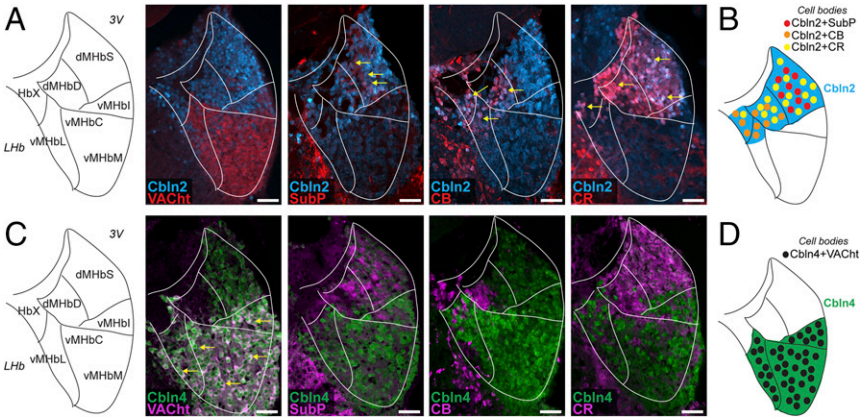

Fig. 2. Expression of Cbln2 and Cbln4 is enriched in largely nonoverlapping subnuclei within the MHb. (*A*) Schematic outline of the subnuclei of the MHb (*Left*), and coronal sections (25 μm thickness) of the MHb from Cbln2-mVenus mice colabeled with antibodies to VAChT, SubP, calbindin (CB), or calretinin (CR). Cbln2 expression was visualized using an endogenous mVenus signal. (*B*) Schematic summarizing the localization of Cbln2-expressing neurons in the MHb (*blue region*) that coexpress SubP (*red circles*), CB (*orange circles*), and CR (*yellow circles*). (*C*) Same as *A* but for Cbln4. Cbln4 expression was visualized using an antibody to GFP to boost the intensity of the mVenus signal. (*D*) Schematic summarizing the localization of Cbln4-expressing neurons in the MHb (*green regions*) that coexpress VAChT (*black circles*). (Scale bars: 50 μm.) 3V, third ventricle.

their differential expression patterns in the MHb, Cbln2$^+$ axons were segregated primarily to the IPL and partially to the IPR and were colabeled with subP, calbindin, and calretinin (Fig. 3 *A* and *B* and *SI Appendix*, Fig. S2*A*). No Cbln2$^+$ axons were observed in the IPC or colabeled with VAChT (Fig. 3*A* and *SI Appendix*, Fig. S2*A*). Conversely, Cbln4$^+$ axons were not observed in the IPL, but fully overlapped with VAChT$^+$ axons in the IPR and IPC (Fig. 3 *C* and *D* and *SI Appendix*, Fig. S2*B*).

Taken together, these results show that Cbln2 and Cbln4 are expressed in neurons of distinct subnuclei of the MHb, and that these neurons send projections to distinct target regions of the IPN.

Loss of Cbln2, but Not of Cbln4, in the MHb Decreases the Frequency of mEPSCs and Causes a Delayed Loss of vGluT1$^+$ Synapses in the IPL. Because cerebellins are thought to be produced presynaptically and to function as transsynaptic organizers (45–48, 53), we next used electrophysiology and immunohistochemistry to assess the effect of conditional Cbln2 or Cbln4 deletions in the MHb on synaptic projections from the MHb to the IPN. In these experiments, we stereotactically injected adeno-associated viruses (AAVs) that express active (Cre) or inactive mutant Cre-recombinase (ΔCre) under control of the synapsin-1 promoter into the MHb of Cbln2 or Cbln4 conditional KO (cKO) mice aged 21–24 d (Fig. 4*A*). We performed electrophysiological recordings from patched neurons in the IPL of Cbln2 cKO mice and in the IPC of Cbln4 cKO mice at 3 wk after injections and analyzed cryosections from injected mice by immunocytochemistry at both 3 wk and ∼3 mo after injections (Fig. 4*A*). In the immunocytochemistry experiments, we quantified the size and density of presynaptic vGluT1$^+$, vGluT2$^+$, and vGAT$^+$ puncta and postsynaptic PSD95$^+$ puncta in the IPL and IPC of both groups of mice to test whether cerebellins may be essential for the initial formation of synapses or whether the deletion of a cerebellin may cause a secondary loss of synapses (Fig. 4 and *SI Appendix*, Figs. S3 and S4).

We found that loss of Cbln2 in the MHb strongly decreased the mEPSC frequency of neurons in its IPL target area (∼70% decrease; Fig. 4 *B* and *C*). We also observed a trend toward a decrease in mEPSC amplitude that was not statistically significant. At the time of these electrophysiological recordings (3 wk after stereotactic injections), we observed no change in the density of vGluT1$^+$ synapses in either the IPL (Fig. 4 *D* and *E*) or the IPC (*SI Appendix*, Fig. S3*B*). However, at ∼3 mo after the stereotactic injections, we detected a significant decrease (∼30%) in both the density and the size of vGluT1$^+$ puncta as well as a decrease

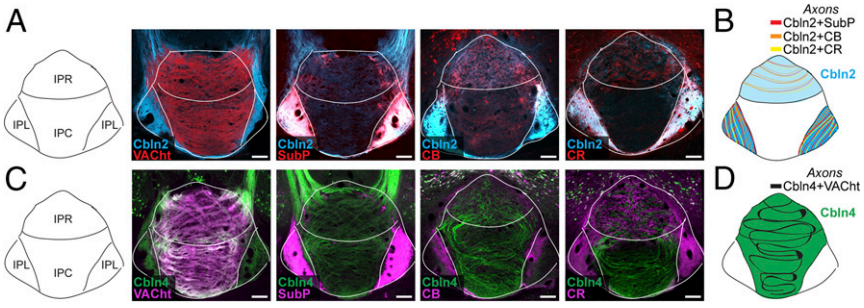

Fig. 3. Axons from Cbln2- and Cbln4-expressing MHb neurons project to distinct subnuclei of the IPN. (*A*) Schematic outlining the subnuclei of the IPN (*Left*) and coronal sections (25 μm thick) of the IPN from Cbln2-mVenus mice. The subregional localization of specific MHb-IPN projections are visualized by colabeling with antibodies against VAChT, SubP, calbindin (CB), or calretinin (CR). Cbln2 expression was visualized using the endogenous mVenus signal. (*B*) Schematic summarizing the localization of subnuclei in the IPN (*blue regions*) that contain Cbln2$^+$ axonal projections from the MHb and that coexpress SubP (*red lines*), CB (*orange lines*), or CR (*yellow lines*). Note that Cbln2$^+$ axons terminate primarily in the IPL region, but also in the IPR region of the IPN. (*C*) Same as *A*, but for Cbln4. Cbln4 expression was visualized using an antibody against GFP to boost the intensity of the mVenus signal. (*D*) Schematic summarizing the localization of subnuclei in the IPN (*green regions*) that contain Cbln4$^+$ axonal projections from the MHb and that coexpress (*black lines*). Note that Cbln4$^+$ axons terminate in the IPR and IPC regions of the IPN. (Scale bars: 200 μm.)

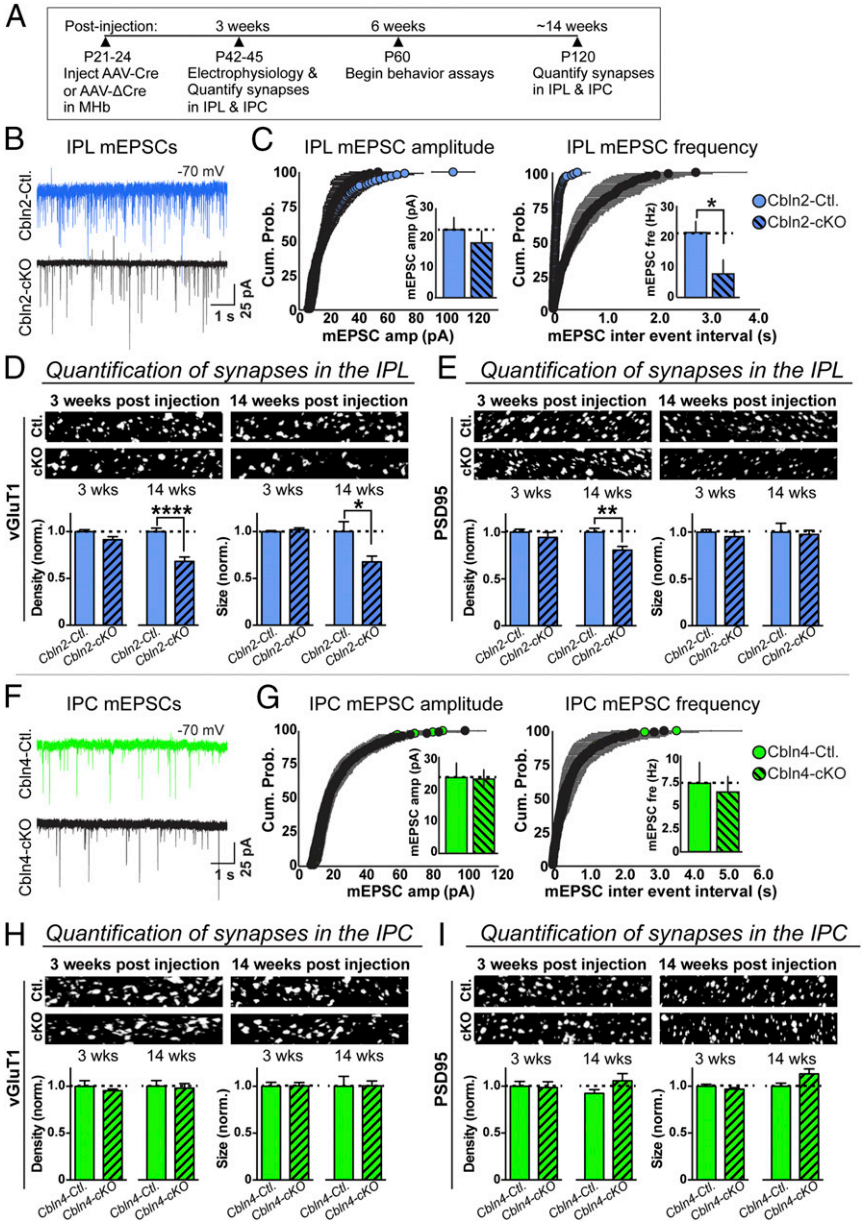

Fig. 4. MHb deletion of Cbln2, but not of Cbln4, causes a rapid decrease in the frequency of spontaneous mEPSCs and a delayed loss of vGluT1$^+$ synapse density in the IPN. (*A*) Experimental strategy. The schematic shows the time course of stereotactic virus injections into the MHb of Cbln2 and Cbln4 cKO mice and of the electrophysiological (3 wk after injections), behavioral (starting 6 wk after injections; Figs. 5 and 6), and morphological (3 and 14 wk after injections) analyses of these mice. Note that all controls were injected with viruses expressing mutant inactive Cre-recombinase (ΔCre), and all analyses were performed on anonymized mice, slices, or sections. (*B* and *C*) Loss of Cbln2 in the MHb decreases the frequency, but not the amplitude, of mEPSCs monitored in IPL neurons at 3 wk after injections. (*B*) Representative traces. (*C*) Summary graphs of the cumulative mEPSC amplitude (*Left, Inset*, mean mEPSC amplitude) and of the cumulative interevent interval (*Right, Inset*, mean mEPSC frequency). Statistical significance was evaluated for cumulative plots using the Kolmogorov–Smirnov test (amplitude, $P = 0.193$; interevent interval: $^{****}P = 0.0001$) and for summary graphs using Student's *t* test (amplitude, $P = 0.44$; frequency, $^{*}P = 0.02$). $n = 8$ cells/4 mice and $n = 7$ cells/4 mice for Cbln2 cKO test and controls, respectively. (*D* and *E*) Loss of Cbln2 in the MHb has no effect on excitatory synapses in the IPL at 3 wk after injections, but selectively decreases the density and size of presynaptic vGluT1$^+$ puncta and the density of postsynaptic PSD95$^+$ puncta in the IPL at ~14 wk after injections. Shown are representative images (*Top*) and summary graphs of the density and size of the vGluT1$^+$ puncta (*D*) or PSD95$^+$ puncta (*E*) at 3 and 14 wk after viral injections into the MHb. Synapse size and density were normalized by the region of interest area and then by the values seen in the controls. Data are mean ± SEM (n = 3 sections/mouse, 3 mice/genotype). Statistical significance was assessed by Student's *t* test. $^{****}P < 0.0001$; $^{**}P = 0.0028$; $^{*}P = 0.0175$. (*F* and *G*) Deletion of Cbln4 in the MHb has no effect on the frequency or amplitude of mEPSCs monitored in IPC neurons at 3 wk after injections. (*F*) Representative traces, (*G*) Summary graphs of the cumulative mEPSC amplitude (*Left, Inset*, mean mEPSC amplitude) and of the cumulative interevent interval (*Right, Inset*, mean mEPSC frequency). Statistical significance was evaluated as described for *B* and *C* (n = 8 cells/4 mice for Cbln4 cKO test and n = 14 cells/4 mice for controls). (*H* and *I*) Same as *D* and *E* but for Cbln4. Loss of Cbln4 in the MHb had no effect on vGluT1$^+$ synapse size or density in the IPL (*H*) or IPC (*I*) at either time point.

(~20%) in the density of PSD95$^+$ puncta. This synapse density decrease was detectable only in the IPL and not in the IPC (Fig. 4 *D* and *E* and *SI Appendix*, Fig. S3*B*). Importantly, this decrease was specific for vGluT1$^+$ synapses, as we found no change in vGluT2$^+$ or vGAT$^+$ puncta in either the IPL or IPC (*SI Appendix*, Fig. S3). Thus, the Cbln2 deletion in the MHb causes a relatively rapid loss

of synaptic efficacy in Cbln2 target synapses of the MHb in the IPN as monitored by mEPSCs, and a delayed selective loss of synapses that is much less severe and restricted to vGluT1$^+$ synapses.

In contrast to the Cbln2 deletion, the Cbln4 conditional deletion had no effect on either mEPSCs at 3 wk after injections or synapse density at 3 wk or ∼3 mo after injections (Fig. 4 *F* and *G*). Specifically, we observed no change in the density or size of vGluT1$^+$, vGluT2$^+$, vGAT$^+$, or PSD95$^+$ puncta in either the IPC or the IPL even at 3 mo after conditional Cbln4 ablation in the MHb (Fig. 4 *H* and *I* and *SI Appendix*, Fig. S4).

MHb Deletion of Cbln4, but Not of Cbln2, Increases Anxiety-Related Behaviors. Lesion experiments and genetic studies in mice, rats, and zebrafish have shown that the MHb-IPN pathway plays a crucial role in anxiety, spatial learning and memory, passive and active avoidance learning, and nicotine consumption (8, 15–17, 19, 21, 54). To determine the function of Cbln2 and Cbln4 in the MHb projections to the IPN in which they are involved, we used AAVs expressing Cre or ΔCre (control) driven by the synapsin promoter to selectively delete Cbln2 or Cbln4 in the MHb (Fig. 5 *A*–*D*), and then tested the mice for changes in select forms of learning, memory, and anxiety.

We initially tested the mice for anxiety-like behaviors using the open field test and the elevated plus maze. In the first experiment, the mice were allowed to freely explore an open field measuring 28 cm long × 28 cm wide × 23.5 cm high for 15 min. General activity and anxiety were assessed by calculating the total distance traveled and time spent in the center of the field, respectively. We observed no differences in distance traveled or time spent in the center of the field in either the Cbln2-cKO (Fig. 5*E*) or Cbln4-cKO (Fig. 5*G*) mice compared with their respective controls.

In the elevated plus maze, we also detected no difference between the Cbln2-Ctl and Cbln2-cKO mice in either the total time spent in the open arms or the latency to first enter the open arms (Fig. 5*F*). In contrast, Cbln4-cKO mice spent ∼60% less time in the open arms, suggesting increased anxiety (Fig. 5*H*), and also exhibited an increased latency to enter the open arms, ∼5-fold greater than that seen in the Cbln4-Ctl mice (numerical data provided in *SI Appendix*, Tables S1 and S2).

Because the Cbln4-cKO mice displayed increased anxiety on the elevated plus maze, we decided to test the mice in a larger (40 × 40 × 40 cm) open field. To entice the mice to venture out into the field, a novel object was placed in the center of the field. We then assayed the mice's latency to enter and total amount of time spent in the center 20 × 20 cm area (whether exploring the object or not). In this assay, the Cbln4-cKO mice again displayed increased anxiety (Fig. 5*I*) by spending ∼43% less time in the center of the open field compared with controls (*SI Appendix*, Table S2). The Cbln4-cKO mice also had an increased latency to enter the center; however, this difference did not reach statistical significance (*SI Appendix*, Table S2).

Finally, because the elevated plus maze and open field tests measure open space anxiety, we wanted to test the specificity of the Cbln4-cKO mice by measuring their anxiety in response to a different type of stressor. To that end, we used the light/dark test to measure the level of anxiety in response to bright light. In this assay, there was no difference between the Cbln4-Ctl mice (n = 11) and Cbln4-cKO mice (n = 10) in either the latency to enter the brightly lit chamber or the total time spent in the lighted chamber (Fig. 5*J* and *SI Appendix*, Table S2). Taken together, these results show that loss of Cbln4, but not loss of Cbln2, in the MHb increases open space anxiety but has no effect on bright light anxiety.

MHb Deletion of Cbln2, but Not of Cbln4, Impairs Passive Avoidance Learning but Not Fear Learning. We next used a light/dark two-chamber shuttle box to measure passive avoidance learning. At baseline, there was no difference between the Cbln2-cKO mice (n = 11) and Cbln2-Ctl mice (n = 11) in exit latency (i.e., time to enter the dark chamber); however, in all four recall trials, the Cbln2-cKO mice had a significantly shorter exit latency than the control mice. Using Sidak's post hoc analysis to correct for multiple comparisons, we found that the Cbln2-Ctl mice exhibited a significantly increased exit latency compared with baseline in recall trials 1–3, but not in recall trial 4 (*SI Appendix*, Table S1). Conversely, the Cbln2-cKO mice did not show increased exit latency compared with baseline in any of the recall trials (Fig. 5*K*). In contrast to the Cbln2-cKO mice, the Cbln4-cKO mice did not show any impairment in passive avoidance learning (Fig. 5*L*) or any difference in baseline exit latency compared with control mice (*SI Appendix*, Table S2).

We next tested conditioned fear learning with contextual and cued recall. Somewhat surprisingly, given the impaired passive avoidance learning phenotype that we observed, the Cbln2-cKO mice were indistinguishable from their control littermates during training, context recall, and cued recall trials (*SI Appendix*, Fig. S5*A* and Table S1). The Cbln4-cKO mice showed a small but significant decrease in freezing behavior during the training trials compared with Cbln4-Ctl mice (*SI Appendix*, Table S2); however, this does not appear to reflect a deficit in learning, because there was no difference between the two groups in the context and cued recall trials (*SI Appendix*, Fig. S5*B*).

MHb Deletion of Cbln2, but Not of Cbln4, Impairs Spatial Learning and Short-Term Memory. We next tested visual spatial learning and reversal learning using a water T-maze. During the learning phase, mice were subjected to 10 trials/day to learn the location of a submerged platform placed in one arm of a T-maze. The time to find the platform and total number of errors (i.e., incorrect arm entries) was recorded for each trial; a successful trial was one in which the mouse was able to find the platform without making an error. Training was completed when the mouse achieved a success rate of ≥80% for 2 consecutive days.

The Cbln2-cKO mice showed significant deficits in spatial learning (Fig. 6*A*), requiring an average of 3 d to complete the training, while their control littermates required an average of 2 d (*SI Appendix*, Table S1). The most significant deficits were observed during the first day of training, during which the Cbln2-cKO mice required ∼50% more time to find the hidden platform compared with the control mice (*SI Appendix*, Table S1).

During the first training day, the Cbln2-cKO mice also made ∼5 times more errors than the Cbln2-Ctl mice and had a mean success rate of 54% compared with the Cbln2-Ctl average success rate of 91% (*SI Appendix*, Table S1). Importantly, the observed increase in escape latency was not due to motor or swimming deficits in the KO mice, because the Cbln2-cKO mice showed an increase in swimming speed (*SI Appendix*, Table S1). This is also consistent with a previous study in which habenula-lesioned rats swam faster than control rats in the Morris water maze, which also tests spatial learning and memory (19).

Following completion of the training phase, the platform was moved to the opposite arm of the maze, and the mice were subjected to 10 trials/d for 2 consecutive days to learn the new location of the platform. The time to find the platform and total errors were recorded for each trial, and the success rate was calculated for each day. During the first day of reversal learning, the Cbln2-cKO mice required less time to find the platform compared with the Cbln2-Ctl mice; however, this was likely due to the increase in swimming speed observed in the KO mice, given the lack of difference between the two groups in the total number of errors and percentage of successful trials on either training day (*SI Appendix*, Fig. S6*A* and Table S1). In contrast to the Cbln2-cKO mice, the Cbln4-cKO mice showed no deficits in spatial learning (Fig. 6*B* and *SI Appendix*, Table S2) or reversal learning (*SI Appendix*, Fig. S6*B*), and their swimming speed did not differ from that of the Cbln4-Ctl mice (n = 12; Fig. 6*B*).

In an effort to replicate the spatial learning deficit observed in the Cbln2-cKO mice in the water T-maze, we next assessed spatial learning using a wading/shallow water (2 cm deep) Barnes maze (*SI Appendix*, Fig. S7*A*). The mice were subjected to 4 trials/d

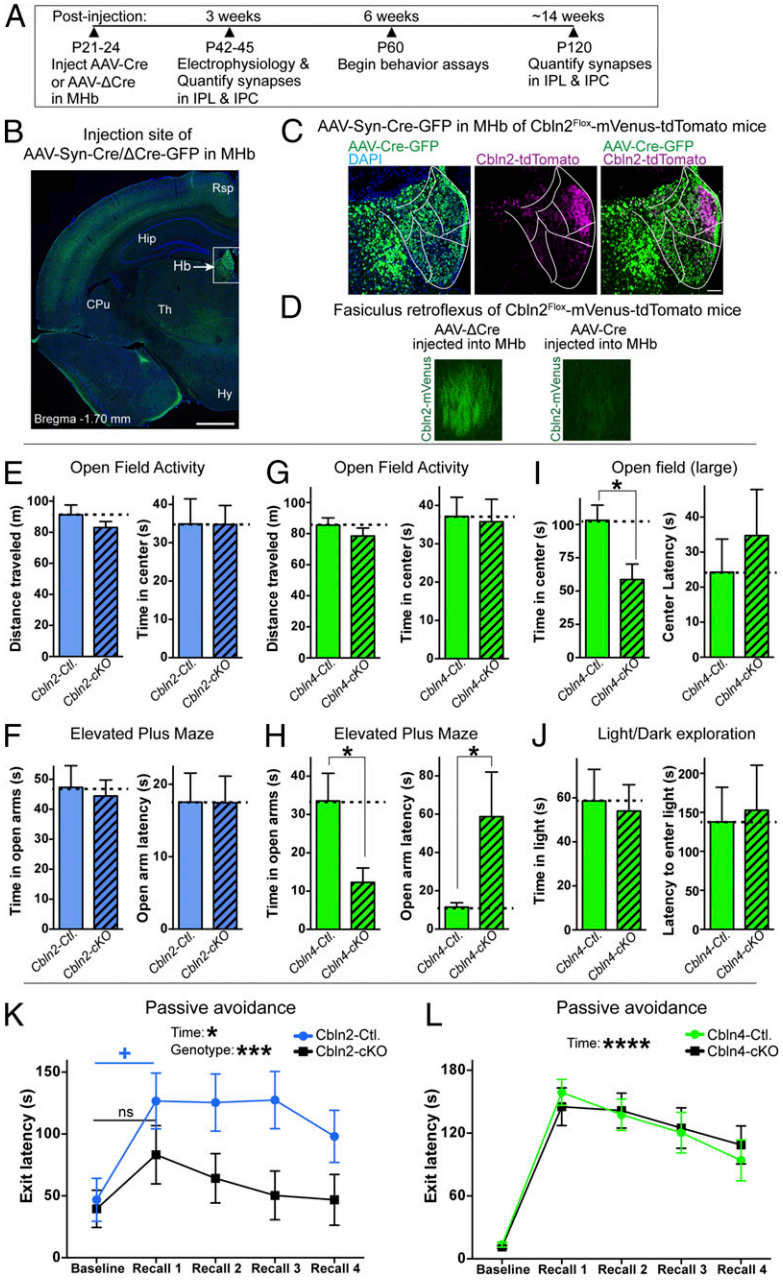

Fig. 5. Deletion of Cbln4 or Cbln2 in the MHb of juvenile mice differentially affects anxiety or passive avoidance learning behaviors. (*A*) Experimental strategy. The schematic shows the time course of stereotactic virus injections into the MHb of Cbln2 and Cbln4 cKO mice and of the electrophysiological, behavioral, and morphological analyses of these mice. (*B*) Representative coronal brain section showing expression of GFP (green) after stereotactic injection of AAV-Syn-Cre-GFP into the MHb. The bregma value denotes the anteroposterior position of the section from bregma in millimeters, as previously described (66). (Scale bar: 1 mm.) (*C*) High-magnification image demonstrating the efficacy of the Cre-mediated recombination following stereotactic injection of AAV-Syn-Cre-GFP (green) into the MHb of Cbln2-mVenus-tdTomato cKO mouse. Neurons in which Cbln2 has been knocked out express tdTomato (false-colored magenta). (Scale bars: 50 μm.) (*D*) Coronal sections showing the fasciculus retroflexus (FR) following stereotactic injection of AAV- ΔCre into the MHb of one hemisphere (*Left*) and AAV-Cre into the MHb of the other hemisphere (*Right*) in a single Cbln2-mVenus-tdTomato cKO mouse. Following Cre-mediated recombination, Cbln2 is deleted from the MHb, resulting in a loss of mVenus expression (green). (Magnification: *D*, 20×.) (*E* and *F*) No change in anxiety-like behavior or general activity in Cbln2-cKO mice ($n = 10$) compared with Cbln2-Ctl mice ($n = 11$) in the open field test (*E*) or elevated plus maze (*F*). (*G*) In an open field measuring 28 × 28 cm, there was no difference in total distance traveled or time spent in the center of the field between the Cbln4-Ctl ($n = 12$) and Cbln4-cKO mice ($n = 10$). (*H*) In an open field measuring 40 × 40 cm, Cbln4-cKO mice ($n = 10$) spent significantly less time in the center of the field (*$P = 0.0135$, Student's *t* test) compared with Cbln4-Ctl mice ($n = 12$), although there was no significant difference between groups in the latency to enter the center of the field. (*I*) In the elevated plus maze, Cbln4-cKO mice ($n = 10$) spent significantly less time in the open arms (*$P = 0.0198$, Student's *t* test), and had an increased latency to enter the open arms (*$P = 0.0471$, Student's *t* test) compared with Cbln4-Ctl mice ($n = 11$). (*J*) In the light/dark exploration test, there was no difference in the total time spent in the light chamber or in the latency to enter the light chamber between Cbln4-Ctl ($n = 12$) and Cbln4-cKO mice ($n = 10$). (*K*) In the passive avoidance test, there was no difference in baseline exit latency (i.e., time to enter the dark chamber) between the Cbln2-Ctl ($n = 11$) and Cbln2-cKO ($n = 11$) mice. During the recall sessions, Cbln2-Ctl mice took significantly more time to enter the dark chamber (i.e., increased exit latency) than at baseline (vs. recall trial 1: $^{+}$adjusted $P = 0.0304$, Sidak's post hoc test), and compared with Cbln2-cKO mice (time, *$P = 0.0344$; genotype, ***$P = 0.0004$, two-way ANOVA), whereas the Cbln2-cKO mice did not significantly increase their escape latency compared with baseline. (*L*) Same as *K* but for Cbln4. There was no difference between Cbln4-Ctl and Cbln4-cKO mice at any time point. and both groups demonstrated learning (time, ****$P < 0.0001$, two-way ANOVA). Data are shown as mean ± SEM.

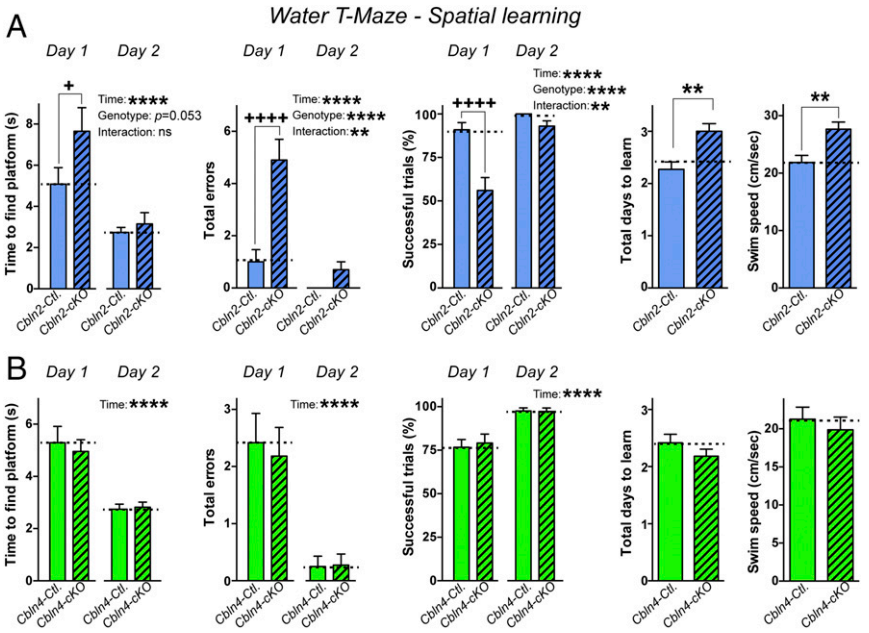

Fig. 6. Deletion of Cbln2, but not of Cbln4, in the MHb impairs spatial learning. (*A*) Compared with control littermates (Cbln2-Ctl; $n = 11$), Cbln2-cKO mice ($n = 10$) showed significant impairment in spatial learning during the acquisition phase of the water T-maze, particularly in the first day of training. Cbln2-cKO mice took significantly more time to find the hidden platform (time, $^{****}P < 0.0001$; genotype, $P = 0.053$, two-way ANOVA; day 1: $^{+}$adjusted $P = 0.0396$, Sidak's post hoc test), made significantly more errors (time, $^{****}P < 0.0001$; genotype, $^{****}P < 0.0001$; interaction, $^{**}P = 0.0017$, two-way ANOVA; day 1: $^{++++}$adjusted $P < 0.0001$, Sidak's post hoc test), completed significantly fewer successful trials (time, $^{****}P < 0.0001$; genotype, $^{****}P < 0.0001$; interaction, $^{**}P = 0.0031$, two-way ANOVA; day 1: $^{++++}$adjusted $P < 0.0001$, Sidak's post hoc test), and required more days overall to complete training ($^{**}P = 0.0021$, Student's *t* test). The Cbln2-cKO mice also displayed increased swimming speed compared with controls ($^{**}P = 0.0034$, Student's *t* test). (*B*) Same as *A* but for Cbln4. The Cbln4-cKO mice ($n = 10$) showed normal spatial learning and memory by performing equally as well as control mice (Cbln4-Ctl; $n = 12$) on the water T-maze. In addition, there was no difference in swimming speed between the two groups. Data are shown as mean ± SEM.

for 4 d to learn the location of a hidden escape tunnel. The escape latency and number of errors (i.e., incorrect nose pokes) were measured during the first and last trials of day 1 (trials 1 and 4, respectively), the last trial of days 3 and 4 (trials 8 and 12, respectively), and the first trial of day 5 (probe trial).

During the first trial (baseline), there was no difference between the Cbln2-Ctl and Cbln2-cKO mice in either the time to find the escape tunnel or the number of errors committed. However, by the end of the first training day (trial 4), the Cbln2-Ctl mice showed significantly improved performance in both time and errors, whereas the Cbln2-cKO mice did not show significant improvements in either time or errors (*SI Appendix*, Fig. S7*A*).

Comparing the groups, the Cbln2-cKO mice required nearly 3.5-fold more time to find the escape tunnel and committed nearly 4-fold more errors during trial 4 than the Cbln2-Ctl mice (*SI Appendix*, Fig. S7*A*). There was no difference in escape latency between the two groups across the remaining learning trials or in the probe trial; however, the Cbln2-cKO mice continued to make more errors on average during the learning trials but not during the probe trial (*SI Appendix*, Fig. S7*A*). Similar to what we observed in the water T-maze, there was no difference between the Cbln2-Ctl and Cbln2-cKO mice during reversal learning in either escape latency or errors (*SI Appendix*, Fig. S7*B*).

Finally, we asked whether the learning deficits observed in the Cbln2-cKO mice were due to general cognitive impairments or specifically to impairment in spatial learning. To test this, the mice were subjected to the novel object recognition test. When presented with a familiar object and a novel object, both the Cbln2-Ctl and Cbln2-cKO mice spent significantly more time exploring the novel object (*SI Appendix*, Fig. S8*A* and Table S1). Similar results were seen in the Cbln4-Ctl and Cbln4-cre mice, with both groups also spending significantly more time exploring the novel object compared with the familiar object (*SI Appendix*, Fig. S8*B* and Table S2).

Taken together, the foregoing results show that loss of Cbln2, but not of Cbln4, in the MHb impairs spatial learning and short-term memory, while general learning and long-term memory remain unaffected.

Discussion

Previous lesion studies using rat, mouse, and zebrafish have established a role for the MHb-IPN pathway in regulating spatial learning and memory, fear acquisition, passive and active avoidance learning, and anxiety (8, 15–17, 19, 21). Moreover, recent work has suggested that regulation of these behaviors is divided between parallel dMHb→lPL and vMHb→lPC pathways (8, 15, 16, 55). The precise function of these pathways and how they are independently regulated remain unknown, however. In the present study, we show that Cbln2 is highly expressed in the dMHb (Figs. 1*B* and 2*A*) and plays an important role in the dMHb-IPL pathway, whereas Cbln4 is highly expressed in the vMHb (Figs. 1*C* and 2*C*) and contributes to the function of the vMHb-IPC pathway, thus delineating molecular determinants for these two parallel neural circuits.

We used qRT-PCR to show that Cbln1, Cbln2, and Cbln4 and their presynaptic binding partners Nrxn1, Nrxn2, and Nrxn3 are abundantly expressed in the habenula complex (Fig. 1*F*). We also demonstrated that in the habenula, neurexins are present primarily as +SS4 isoforms capable of binding to cerebellins (Fig. 1*G*), and that the postsynaptic Cbln2-binding partners *Grid1* and *Grid2* (which encode GluRδ1 and GluRδ2, respectively) and the Cbln4-binding partners *DCC* and *NEO1* are produced in the IPN (Fig. 1*H*). These results show that in principle, Cbln2 could function in the dMHb-IPL pathway by mediating transsynaptic interactions between presynaptic neurexin +SS4 isoforms expressed in dMHb neurons and postsynaptic GluRδ1/2 expressed in IPL neurons. Conversely, Cbln4 could function in the vMHb-IPC pathway by mediating an interaction between presynaptic neurexin +SS4

isoforms expressed in vMHb neurons and DCC/NEO1 or other unknown binding partners in postsynaptic IPC neurons.

We found that genetic deletion of Cbln2 in the MHb of adult mice (P21–P24) resulted in an ∼60% reduction in mEPSC frequency in the dMHb target IPL neurons but not in IPC neurons, as assessed at 3 wk after the deletion (Fig. 4 *B* and *C*). Despite this dramatic reduction in mEPSC frequency, we detected no changes in synapse numbers or synapse size at this time point. However, we observed an ∼30% reduction in the density and size of excitatory presynaptic vGluT1$^+$ puncta, as well as an ∼20% reduction in the density of postsynaptic PSD95$^+$ puncta in the IPL (but again not in the IPC) at 3 mo after the Cbln2 deletion (Fig. 4 *D* and *E*). We detected no changes in excitatory vGluT2$^+$ or inhibitory vGAT$^+$ puncta in the IPL or IPC (*SI Appendix*, Fig. S3). These results suggest that the Cbln2 deletion impaired synapse function, and that this impairment caused a delayed secondary loss of synapses. These results are thus consistent with our hypothesis that cerebellins are involved in synapse specification and long-term synapse stabilization but not in establishing synapses (44, 48).

Genetic deletion of Cbln4 in the MHb did not produce any changes in mEPSC frequency or amplitude in IPC or IPL neurons (Fig. 4 *F* and *G*), and also did not alter the density or size of excitatory vGluT1$^+$ or vGluT2$^+$ or inhibitory vGAT$^+$ synapses (Fig. 4 *H* and *I* and *SI Appendix*, Fig. S4). These findings are surprising considering the behavioral phenotype that we observed in these mice, which suggests that Cbln4 is functionally important to the vMHb-IPC pathway. Previous work from our laboratory and other authors has also failed to identify phenotypes of Cbln4 deletions in the adult brain (36, 37, 48). Future research will need to answer the important question of what precisely Cbln4 does in synapses, and the vMHb-IPC pathway may serve as an expedient circuit in which to address this question.

Importantly, mice carrying selective MHb deletions of Cbln2 or Cbln4 exhibited major but different behavioral changes. Specifically, Cbln2 deletions produced significant impairments in spatial learning and short-term memory as analyzed in the water T-maze and wading Barnes maze (Fig. 6*A* and *SI Appendix*, Fig. S7*A*), whereas Cbln4 deletions had no effect on spatial learning (Fig. 6*B*). In addition, Cbln2 cKO mice displayed significantly impaired passive avoidance learning, while the Cbln4 cKO mice did not (Fig. 5 *K* and *L*). This result agrees well with earlier reports showing impaired avoidance learning in habenula-lesioned rats (21, 22).

Our data are also consistent with a recent study in which researchers used immunotoxin-mediated cell targeting to selectively ablate neurons in the triangular septum that project to the vMHb or neurons in the bed nucleus of the anterior commissure (BAC) that project to the dMHb (8). That study found that disruption of the triangular septum inputs into the vMHb increased anxiety but had no effect on fear acquisition or avoidance learning, whereas disruption of the BAC-dMHb inputs had no effect on anxiety but resulted in increased freezing immediately after a foot shock and enhanced avoidance learning (8).

We also observed that the Cbln2-cKO mice swam faster than control mice in the water T-maze (Fig. 6*A*), which is consistent with a previous study in which habenula-lesioned rats swam faster than control rats in the Morris water maze, another test of spatial learning and memory (19). That study suggested that habenula-lesioned rats may be hyperreactive to stress. This idea is supported by another study in which habenula-lesioned rats showed impaired active avoidance learning only when the effort of the operant response and the intensity of the foot shock were high (high stress); avoidance learning was unaffected under low-stress conditions, suggesting that the habenula-lesioned rats were more sensitive to stress-induced learning impairments (21). Supporting this hypothesis, another study found that lesions of the fasciculus retroflexus resulted in chronically elevated plasma levels of corticosterone in rats (56). Taken together, the foregoing results suggest that a general function of the MHb is to regulate the ability of an animal to learn and make decisions under stress, and that Cbln2 may play an important role in mediating this function.

In contrast to the Cbln2 cKO mice, the Cbln4 cKO mice showed increased open space anxiety as measured by the open field test (Fig. 5*I*) and elevated plus maze (Fig. 5*H*), but no change in bright-light anxiety as measured by the light/dark exploration test (Fig. 5*J*), whereas Cbln2 cKO mice exhibited no changes in anxiety during any test (Fig. 5 *E* and *F*). These results are consistent with previous research showing increased anxiety in mice following selective ablation or manipulation of the cholinergic neurons in the vMHb (15, 16).

Taken together, our results suggest that loss of Cbln2 in the dMHb disrupts some forms of hippocampal-dependent learning (avoidance learning and spatial navigation), while leaving other forms of hippocampal-dependent learning intact (contextual fear learning), and that loss of Cbln4 in the vMHb has no effect on hippocampal-dependent learning but increases open space anxiety. These findings are reminiscent of the functional division between the dorsal and ventral hippocampus. For example, lesions to the dorsal, but not the ventral, hippocampus impair spatial learning in rats (57–60), whereas lesions to the ventral, but not the dorsal, hippocampus decrease anxiety-like behaviors (61) and disrupt fear conditioning (62, 63).

These findings suggest two important ideas: (*i*) spatial learning and contextual fear conditioning have different, albeit analogous, underlying neural mechanisms, which may explain why the Cbln2 cKO mice have deficits in spatial learning but not fear-conditioning, and (*ii*) the dorsal hippocampus has a preferential role in spatial learning and memory, while the ventral hippocampus has a preferential role in anxiety- and fear-related behaviors (reviewed in ref. 64). Therefore, the functional divisions in the MHb that we observed may reflect differences in specific inputs to the dMHb and vMHb. Future studies will need to examine the functional significance of the input/output relationship of these brain regions more carefully.

Overall, our results show that the functional compartmentalization of the MHb into dMHb and vMHb subdivisions corresponds to the differential expression patterns of Cbln2 and Cbln4, and that projections from the Cbln2$^+$ and Cbln4$^+$ neurons in the dMHb and vMHb are segregated to the IPL and IPC subdivisions of the IPN, respectively. Deletion of Cbln2 in the MHb disrupts the function of the dMHb-IPL pathway, resulting in impaired avoidance and spatial learning and memory, while deletion of Cbln4 in the MHb disrupts the function of the vMHb-IPC pathway, resulting in increased open space anxiety. Taken together, our data show that Cbln2 and Cbln4 contribute to the functions of parallel pathways involved in learning, memory, and emotion.

Materials and Methods

Animals. All experiments were conducted using adult male Cbln2 and Cbln4 floxed IRES-mVenus-IRES-tdTomato reporter mice maintained on a hybrid C57/Bl6 background, as described previously (29). The colabeling and expression experiments were conducted using 3-wk-old Cbln2-mVenus or Cbln4-mVenus mice. The synapse quantification experiments were conducted using Cbln2-mVenus or Cbln4-mVenus mice aged 3 wk (P42–P45) or ∼14 wk (∼4 mo) following injection of AAV-DJ-Syn-dCRE-GFP or AAV-DJ-Syn-CRE-GFP in the MHb. All animal procedures conformed to National Institutes of Health's *Guide for the Care and Use of Laboratory Animals* (65) and were approved by the Stanford University Administrative Panel on Laboratory Animal Care.

Mouse Behavior. All behavior experiments were conducted using male littermates aged 2–4 mo following injection of AAV-DJ-Syn-dCRE or AAV-DJ-Syn-CRE in the MHb at P21–P24. All behavior assays were conducted and analyzed by researchers who were blinded to genotype.

More detailed descriptions of methods are provided in *SI Appendix, Materials and Methods*.

ACKNOWLEDGMENTS. This study was supported by National Institute of Mental Health Grant MH052804 (to T.C.S.).

1. Herkenham M, Nauta WJ (1977) Afferent connections of the habenular nuclei in the rat: A horseradish peroxidase study, with a note on the fiber-of-passage problem. *J Comp Neurol* 173:123–146.
2. Herkenham M, Nauta WJ (1979) Efferent connections of the habenular nuclei in the rat. *J Comp Neurol* 187:19–47.
3. Aizawa H, Kobayashi M, Tanaka S, Fukai T, Okamoto H (2012) Molecular characterization of the subnuclei in rat habenula. *J Comp Neurol* 520:4051–4066.
4. Raisman G (1966) The connexions of the septum. *Brain* 89:317–348.
5. Swanson LW, Cowan WM (1979) The connections of the septal region in the rat. *J Comp Neurol* 186:621–655.
6. Krayniak PF, Weiner S, Siegel A (1980) An analysis of the efferent connections of the septal area in the cat. *Brain Res* 189:15–29.
7. Qin C, Luo M (2009) Neurochemical phenotypes of the afferent and efferent projections of the mouse medial habenula. *Neuroscience* 161:827–837.
8. Yamaguchi T, Danjo T, Pastan I, Hikida T, Nakanishi S (2013) Distinct roles of segregated transmission of the septo-habenular pathway in anxiety and fear. *Neuron* 78:537–544.
9. Contestabile A, et al. (1987) Topography of cholinergic and substance P pathways in the habenulo-interpeduncular system of the rat: An immunocytochemical and microchemical approach. *Neuroscience* 21:253–270.
10. Baisden RH, Hoover DB, Cowie RJ (1979) Retrograde demonstration of hippocampal afferents from the interpeduncular and reuniens nuclei. *Neurosci Lett* 13:105–109.
11. Shibata H, Suzuki T (1984) Efferent projections of the interpeduncular complex in the rat, with special reference to its subnuclei: A retrograde horseradish peroxidase study. *Brain Res* 296:345–349.
12. Montone KT, Fass B, Hamill GS (1988) Serotonergic and nonserotonergic projections from the rat interpeduncular nucleus to the septum, hippocampal formation and raphe: A combined immunocytochemical and fluorescent retrograde labelling study of neurons in the apical subnucleus. *Brain Res Bull* 20:233–240.
13. Ohara S, Sato S, Tsutsui K, Witter MP, Iijima T (2013) Organization of multisynaptic inputs to the dorsal and ventral dentate gyrus: Retrograde trans-synaptic tracing with rabies virus vector in the rat. *PLoS One* 8:e78928.
14. Lima LB, et al. (2017) Afferent and efferent connections of the interpeduncular nucleus with special reference to circuits involving the habenula and raphe nuclei. *J Comp Neurol* 525:2411–2442.
15. Kobayashi Y, et al. (2013) Genetic dissection of medial habenula-interpeduncular nucleus pathway function in mice. *Front Behav Neurosci* 7:17.
16. Pang X, et al. (2016) Habenula cholinergic neurons regulate anxiety during nicotine withdrawal via nicotinic acetylcholine receptors. *Neuropharmacology* 107:294–304.
17. Agetsuma M, et al. (2010) The habenula is crucial for experience-dependent modification of fear responses in zebrafish. *Nat Neurosci* 13:1354–1356.
18. Thornton EW, Davies C (1991) A water-maze discrimination learning deficit in the rat following lesion of the habenula. *Physiol Behav* 49:819–822.
19. Lecourtier L, Neijt HC, Kelly PH (2004) Habenula lesions cause impaired cognitive performance in rats: Implications for schizophrenia. *Eur J Neurosci* 19:2551–2560.
20. Lecourtier L, Saboureau M, Kelly CD, Pévet P, Kelly PH (2005) Impaired cognitive performance in rats after complete epithalamus lesions, but not after pinealectomy alone. *Behav Brain Res* 161:276–285.
21. Thornton EW, Bradbury GE (1989) Effort and stress influence the effect of lesion of the habenula complex in one-way active avoidance learning. *Physiol Behav* 45: 929–935.
22. Thornton EW, Murray M, Connors-Eckenrode T, Haun F (1994) Dissociation of behavioral changes in rats resulting from lesions of the habenula versus fasciculus retroflexus and their possible anatomical substrates. *Behav Neurosci* 108:1150–1162.
23. Clark BJ, Taube JS (2009) Deficits in landmark navigation and path integration after lesions of the interpeduncular nucleus. *Behav Neurosci* 123:490–503.
24. Pang Z, Zuo J, Morgan JI (2000) Cbln3, a novel member of the precerebellin family that binds specifically to Cbln1. *J Neurosci* 20:6333–6339.
25. Bao D, et al. (2006) Cbln1 is essential for interaction-dependent secretion of Cbln3. *Mol Cell Biol* 26:9327–9337.
26. Miura E, Iijima T, Yuzaki M, Watanabe M (2006) Distinct expression of Cbln family mRNAs in developing and adult mouse brains. *Eur J Neurosci* 24:750–760.
27. Wei P, Smeyne RJ, Bao D, Parris J, Morgan JI (2007) Mapping of Cbln1-like immunoreactivity in adult and developing mouse brain and its localization to the endolysosomal compartment of neurons. *Eur J Neurosci* 26:2962–2978.
28. Otsuka S, et al. (2016) Roles of Cbln1 in non-motor functions of mice. *J Neurosci* 36: 11801–11816.
29. Seigneur E, Südhof TC (2017) Cerebellins are differentially expressed in selective subsets of neurons throughout the brain. *J Comp Neurol* 525:3286–3311.
30. Ito-Ishida A, et al. (2008) Cbln1 regulates rapid formation and maintenance of excitatory synapses in mature cerebellar Purkinje cells *in vitro* and *in vivo*. *J Neurosci* 28: 5920–5930.
31. Uemura T, et al. (2010) Trans-synaptic interaction of GluRdelta2 and Neurexin through Cbln1 mediates synapse formation in the cerebellum. *Cell* 141:1068–1079.
32. Matsuda K, Yuzaki M (2011) Cbln family proteins promote synapse formation by regulating distinct neurexin signaling pathways in various brain regions. *Eur J Neurosci* 33:1447–1461.
33. Lee SJ, Uemura T, Yoshida T, Mishina M (2012) GluRδ2 assembles four neurexins into trans-synaptic triad to trigger synapse formation. *J Neurosci* 32:4688–4701.
34. Cheng S, Seven AB, Wang J, Skiniotis G, Özkan E (2016) Conformational plasticity in the transsynaptic neurexin-cerebellin-glutamate receptor adhesion complex. *Structure* 24:2163–2173.
35. Zhong C, et al. (2017) Cbln1 and Cbln4 are structurally similar but differ in GluD2-binding interactions. *Cell Rep* 20:2328–2340.
36. Wei P, et al. (2012) The Cbln family of proteins interact with multiple signaling pathways. *J Neurochem* 121:717–729.
37. Haddick PC, et al. (2014) Defining the ligand specificity of the deleted in colorectal cancer (DCC) receptor. *PLoS One* 9:e84823.
38. Ushkaryov YA, Petrenko AG, Geppert M, Südhof TC (1992) Neurexins: Synaptic cell surface proteins related to the α-latrotoxin receptor and laminin. *Science* 257:50–56.
39. Ushkaryov YA, et al. (1994) Conserved domain structure of beta-neurexins: Unusual cleaved signal sequences in receptor-like neuronal cell-surface proteins. *J Biol Chem* 269:11987–11992.
40. Ushkaryov YA, Südhof TC (1993) Neurexin III α: Extensive alternative splicing generates membrane-bound and soluble forms. *Proc Natl Acad Sci USA* 90:6410–6414.
41. Ullrich B, Ushkaryov YA, Südhof TC (1995) Cartography of neurexins: More than 1000 isoforms generated by alternative splicing and expressed in distinct subsets of neurons. *Neuron* 14:497–507.
42. Treutlein B, Gokce O, Quake SR, Südhof TC (2014) Cartography of neurexin alternative splicing mapped by single-molecule long-read mRNA sequencing. *Proc Natl Acad Sci USA* 111:E1291–E1299.
43. Schreiner D, et al. (2014) Targeted combinatorial alternative splicing generates brain region-specific repertoires of neurexins. *Neuron* 84:386–398.
44. Südhof TC (2017) Synaptic neurexin complexes: A molecular code for the logic of neural circuits. *Cell* 171:745–769.
45. Yuzaki M (2009) New (but old) molecules regulating synapse integrity and plasticity: Cbln1 and the δ2 glutamate receptor. *Neuroscience* 162:633–643.
46. Hirai H, et al. (2005) Cbln1 is essential for synaptic integrity and plasticity in the cerebellum. *Nat Neurosci* 8:1534–1541.
47. Rong Y, et al. (2012) Comparison of Cbln1 and Cbln2 functions using transgenic and knockout mice. *J Neurochem* 120:528–540.
48. Seigneur E, Südhof TC (2018) Genetic ablation of all cerebellins reveals synapse organizer functions in multiple regions throughout the brain. *J Neurosci* 38:4774–4790.
49. Aoto J, Martinelli DC, Malenka RC, Tabuchi K, Südhof TC (2013) Presynaptic neurexin-3 alternative splicing trans-synaptically controls postsynaptic AMPA receptor trafficking. *Cell* 154:75–88.
50. Andres KH, von Düring M, Veh RW (1999) Subnuclear organization of the rat habenular complexes. *J Comp Neurol* 407:130–150.
51. Wagner F, French L, Veh RW (2016) Transcriptomic-anatomic analysis of the mouse habenula uncovers a high molecular heterogeneity among neurons in the lateral complex, while gene expression in the medial complex largely obeys subnuclear boundaries. *Brain Struct Funct* 221:39–58.
52. Wagner F, Stroh T, Veh RW (2014) Correlating habenular subnuclei in rat and mouse by using topographic, morphological, and cytochemical criteria. *J Comp Neurol* 522: 2650–2662.
53. Kusnoor SV, Parris J, Muly EC, Morgan JI, Deutch AY (2010) Extracerebellar role for Cerebellin1: Modulation of dendritic spine density and synapses in striatal medium spiny neurons. *J Comp Neurol* 518:2525–2537.
54. Frahm S, et al. (2011) Aversion to nicotine is regulated by the balanced activity of β4 and α5 nicotinic receptor subunits in the medial habenula. *Neuron* 70:522–535.
55. Hsu Y-W, Morton G, Guy EG, Wang SD, Turner EE (2016) Dorsal medial habenula regulation of mood-related behaviors and primary reinforcement by tachykinin-expressing habenula neurons. *eNeuro* 3:e0109–e0116.
56. Murphy CA, DiCamillo AM, Haun F, Murray M (1996) Lesion of the habenular efferent pathway produces anxiety and locomotor hyperactivity in rats: A comparison of the effects of neonatal and adult lesions. *Behav Brain Res* 81:43–52.
57. Moser E, Moser MB, Andersen P (1993) Spatial learning impairment parallels the magnitude of dorsal hippocampal lesions, but is hardly present following ventral lesions. *J Neurosci* 13:3916–3925.
58. Hock BJ, Jr, Bunsey MD (1998) Differential effects of dorsal and ventral hippocampal lesions. *J Neurosci* 18:7027–7032.
59. Bannerman DM, et al. (2002) Double dissociation of function within the hippocampus: Spatial memory and hyponeophagia. *Behav Neurosci* 116:884–901.
60. Pothuizen HH, Zhang WN, Jongen-Rêlo AL, Feldon J, Yee BK (2004) Dissociation of function between the dorsal and the ventral hippocampus in spatial learning abilities of the rat: A within-subject, within-task comparison of reference and working spatial memory. *Eur J Neurosci* 19:705–712.
61. Bannerman DM, et al. (2003) Ventral hippocampal lesions affect anxiety but not spatial learning. *Behav Brain Res* 139:197–213.
62. Maren S, Aharonov G, Fanselow MS (1997) Neurotoxic lesions of the dorsal hippocampus and Pavlovian fear conditioning in rats. *Behav Brain Res* 88:261–274.
63. Richmond MA, et al. (1999) Dissociating context and space within the hippocampus: Effects of complete, dorsal, and ventral excitotoxic hippocampal lesions on conditioned freezing and spatial learning. *Behav Neurosci* 113:1189–1203.
64. Bannerman DM, et al. (2004) Regional dissociations within the hippocampus: Memory and anxiety. *Neurosci Biobehav Rev* 28:273–283.
65. National Research Council (2011) *Guide for the Care and Use of Laboratory Animals* (National Academies Press, Washington, DC), 8th Ed.
66. Paxinos G, Franklin KBJ (2001) *The Mouse Brain in Stereotaxic Coordinates* (Academic, San Diego), 2nd Ed.